A&A 605, A33 (2017)
DOI: 10.1051/0004-6361/201731330

Astronomy & Astrophysics

Analytic mean-field α^2-dynamo with a force-free corona

Alfio Bonanno[1] and Fabio Del Sordo[2,3]

[1] INAF-Osservatorio Astrofisico di Catania, 95125 Catania, Italy
e-mail: alfio.bonanno@oact.inaf.it
[2] Department of Geology & Geophysics, Yale University, New Haven, CT 06511, USA
[3] Nordita, Royal Institute of Technology and Stockholm University, 10691 Stockholm, Sweden
e-mail: fabio@nordita.org

Received 7 June 2017 / Accepted 24 July 2017

ABSTRACT

Context. Stellar dynamos are affected by boundary conditions imposed by stellar coronae. Under some approximations, it is possible to find analytical solutions. Interior dynamo models often consider a current-free corona without taking into account the constraints imposed by the presence of currents in the corona.
Aims. We aim to analytically evaluate the effect of coronal currents and of an outer boundary condition on the efficiency of an α^2 dynamo. We intend to estimate the change in geometry and dynamo excitation numbers with respect to the current-free case.
Methods. We analytically solved the turbulent dynamo induction equation for a homogeneous, non-mirror symmetric turbulence in a spherical domain surrounded by a linear force-free corona with the mean magnetic field $\boldsymbol{B}$ satisfying $\nabla \times \boldsymbol{B} = \beta \boldsymbol{B}$.
Results. The dynamo number is a decreasing function of β. Moreover, if the current is parallel to the field ($\beta > 0$), the dynamo number is smaller than in the force-free case. In contrast, for ($\beta < 0$), the dynamo number is greater than in the force-free case.
Conclusions. Currents in the corona need to be taken into account because they affect the condition for excitation of a dynamo.

Key words. dynamo – stars: coronae – stars: magnetic field

1. Introduction

A consistent description of the magnetic coupling between a magnetized coronal field and a dynamo-generated interior model is still lacking. Mean-field models usually employ a current-free description of the coronal field (Krause & Raedler 1980; Moffatt 1980), an assumption that is not compatible with an active corona.

However, direct numerical simulations are not able to resolve the surface layers where the pressure scale height is very small and the Lorentz force cannot be neglected. Nonetheless, recent models have been used to estimate the effect of a nearly force-free corona on controlling the emergence of flux from lower layers (Warnecke et al. 2011), on the injection of magnetic twist in the heliosphere (Warnecke et al. 2012), and on a global dynamo (e.g., Warnecke et al. 2016), concluding that the presence of a corona cannot be neglected.

Common models of coronal field based on a potential field (Nash et al. 1988),

$$\nabla^2 \boldsymbol{b} = 0, \tag{1}$$

or on a force-free field,

$$\nabla \times \boldsymbol{b} = \beta\, \boldsymbol{b}, \tag{2}$$

where $\boldsymbol{b}$ is the total magnetic field and $\beta = \beta(\boldsymbol{x})$ is a scalar function, are often used to describe chromospheric observations (Wiegelmann & Sakurai 2012). On the other hand, the coupling with the interior is always neglected. In the framework of mean-field dynamo theory, a new proposal has been presented in Bonanno (2016), where a consistent coupling with an $\alpha^2\Omega$ dynamo model for the interior was achieved under the assumption that the coronal field is harmonic. On the other hand, there are no known analytical solutions in spherical symmetry of a dynamo-generated interior field coupled with a force-free exterior. The aim of this paper is to present such a solution for a linear force-free field. Although our solution has been obtained for a very idealized case (non-helical homogeneous turbulence), some of its features are in agreement with the findings of Bonanno (2016).

Moreover, as is well known, in order to obtain the photospheric field from Zeeman-Doppler imaging (ZDI), it is necessary to solve the strongly nonlinear inverse problem. This problem is very often beset by the presence of several local minima. The choice of a proper forward model is therefore essential to make sure we only consider solutions that are physically meaningful (Carroll et al. 2009; Stift & Leone 2017). We therefore hope that our analytical solution can also be useful in the ZDI reconstruction approach.

The structure of this article is the following: Sect. 1 contains the physical motivation of this work, Sect. 2 contains the basic equations of the model and their physical implications, and Sect. 3 is devoted to the conclusions.

2. Model

2.1. Basic equations

We assume that the field in the stellar interior admits a description in terms of the standard mean-field dynamo equation.

In the case of homogeneous, isotropic, and non-mirrorsymmetric turbulence, we can write the evolution equation for the mean magnetic field $\boldsymbol{B}$

$$\frac{\partial \boldsymbol{B}}{\partial t} = \nabla \times (\boldsymbol{U} \times \boldsymbol{B} + \alpha \boldsymbol{B}) - \nabla \times (\eta \nabla \times \boldsymbol{B}), \tag{3}$$

where α describes the turbulent flow, $\boldsymbol{U}$ is the mean flow, and η characterizes the turbulent (eddy) diffusivity. α and η are simple coefficients in our case, but they would be tensors if isotropy were not assumed. A mean field in a turbulent medium is defined as the expectation value of the total field in an ensemble of identical systems. In our case, the mean magnetic field can be seen as a time average of the total magnetic field over a timescale that is shorter than the long-term evolution of the field.

If $\boldsymbol{U} = 0$, we have α = const., η = const., so an exact stationary solution can be obtained by employing the standard decomposition in toroidal and poloidal component

$$\boldsymbol{B} = -\boldsymbol{r} \times \nabla\Psi - \nabla \times (\boldsymbol{r} \times \nabla\Phi) \equiv \boldsymbol{B}_\mathrm{T} + \boldsymbol{B}_\mathrm{P}, \tag{4}$$

where $\Psi = \Psi(r, \vartheta, \varphi)$ and $\Phi = \Phi(r, \vartheta, \varphi)$ are scalar functions, $\boldsymbol{B}_\mathrm{T}$ is the toroidal component, and $\boldsymbol{B}_\mathrm{P}$ is the poloidal component (see Krause & Raedler 1980, for details). By inserting Eqs. (4) in (3), we easily find

$$\frac{\alpha}{\eta}\Psi + \nabla^2\Phi = 0, \tag{5a}$$

$$\nabla^2\left(\frac{\alpha}{\eta}\Phi - \Psi\right) = 0, \tag{5b}$$

which implies

$$\nabla^2\Psi + \left(\frac{\alpha}{\eta}\right)^2 \Psi = 0. \tag{6}$$

It is convenient to employ the following decomposition:

$$\Phi = R \sum_{n=1}^{\infty} \sum_{m=-n}^{m=n} \phi_{mn}(x) Y_n^m(\theta, \varphi) \tag{7a}$$

$$\Psi = \sum_{n=1}^{\infty} \sum_{m=-n}^{m=n} \psi_{mn}(x) Y_n^m(\theta, \varphi), \tag{7b}$$

where x is the normalized stellar radius $x = r/R$, $\phi_{nm}(x)$ and $\psi_{nm}(x)$ are the eigenfunctions of the radial elliptic problem defined by Eq. (5), and $Y_n^m(\vartheta, \varphi)$ are the spherical harmonics functions.

By inserting Eqs. (7b) in (6), we obtain that the only regular interior solution is

$$\psi_{nm}(x) = A_{nm} \frac{J_{n+1/2}(C_\alpha x)}{\sqrt{x}}, \tag{8}$$

where $J_n(x)$ is the Bessel function of the first kind, and A_{nm} is a complex coefficient that must be determined assuming an exterior field configuration. For simplicity's sake, we use $A_{nm} = 1$ whenever we need to normalize quantities such as the mean magnetic field $\boldsymbol{B}$ and the magnetic helicity $\boldsymbol{A} \cdot \boldsymbol{B}$. By substituting Eqs. (8) in (5b), we find (Krause & Raedler 1980)

$$\phi_{nm}(x) = A_{nm} \frac{J_{n+1/2}(C_\alpha x)}{C_\alpha \sqrt{x}} + B_{nm} x^n, \tag{9}$$

where B_{nm} is a constant, and $C_\alpha = \alpha/\eta$ is the eigenvalue parameter of Eq. (5).

2.2. Adding a force-free corona

We now consider that the dynamo domain is surrounded by a corona. In the exterior, we therefore assume that the field satisfies the linear force-free condition, namely Eq. (2) with β = const. This is the state of minimum dissipation for a given amount of magnetic energy (Chandrasekhar & Woltjer 1958). As explained in Chandrasekhar & Kendall (1957), the general solution of Eq. (2) can be obtained by inserting Eqs. (4) in (2), thus obtaining the Helmholtz equation for the Φ function

$$\nabla^2\Phi + \beta^2\Phi = 0, \tag{10}$$

and $\Psi = \beta\Phi$ in this case. The general solution of Eq. (10) reads

$$\Phi = R \sum_{n=1}^{\infty} \sum_{m=-n}^{m=n} [C_{nm} j_n(C_\beta x) + D_{nm} y_n(C_\beta x)] Y_n^m(\theta, \varphi), \tag{11}$$

where $C_\beta = \beta R$, C_{nm} and D_{nm} are coefficients depending on n and m, and $j_n(x)$ and $y_n(x)$ are the spherical Bessel functions:

$$j_n(x) = \sqrt{\frac{\pi}{2x}} J_{n+1/2}(x), \quad y_n(x) = \sqrt{\frac{\pi}{2x}} Y_{n+1/2}(x), \tag{12}$$

where $J_n(x)$, $Y_n(x)$ are the Bessel function of the first and second kind, respectively. We note that as $r \geq R$, differently from what was discussed in Nakagawa (1973) and Priest (1982), the general solution of the linear force-free equations must include both the Bessel function of the first and second kind.

We impose the continuity of all the field components across the boundary, so that

$$[[\boldsymbol{B}]] = 0, \tag{13}$$

where the notation $[[F]]$ indicates the difference between the values assumed by the quantity F on the two different sides of the boundary. This condition implies that

$$[[\boldsymbol{n} \cdot \boldsymbol{B}]] = 0, \quad [[\boldsymbol{n} \cdot \boldsymbol{J}]] = 0, \tag{14}$$

where $\boldsymbol{J}$ is the current, and $\boldsymbol{n}$ is a unit vector perpendicular to the boundary. The continuity of the tangential component of the electric field $\boldsymbol{E}$ reads

$$0 = [[\boldsymbol{n} \times \boldsymbol{E}]] = -[[\boldsymbol{n} \times \alpha\boldsymbol{B}]] + [[\boldsymbol{n} \times \eta\nabla \times \boldsymbol{B}]]. \tag{15}$$

In our case, Eq. (15) reads

$$0 = -\alpha_-(\boldsymbol{n} \times \boldsymbol{B})_- + \eta_-(\boldsymbol{n} \times \nabla \times \boldsymbol{B})_- - \eta_+\beta_+(\boldsymbol{n} \times \boldsymbol{B})_+, \tag{16}$$

which can be satisfied as long as η is not assumed to be infinite in the $r > R$ domain (see P. H. Roberts in Proctor & Gilbert 1994).

After some algebra, it is finally possible to show that the continuity of the field components determines B_{nm}, C_{nm} and D_{nm} as a function of A_{nm} as follows:

$$B_{nm} = \frac{A_{nm}(C_\alpha - C_\beta) J_{n+\frac{1}{2}}(C_\alpha)}{C_\alpha C_\beta} \tag{17a}$$

$$C_{nm} = \frac{\pi A_{nm}}{2} \left(J_{n+\frac{1}{2}}(C_\alpha) J_{n+\frac{3}{2}}(C_\beta) - J_{n+\frac{3}{2}}(C_\alpha) J_{n+\frac{1}{2}}(C_\beta) \right) \tag{17b}$$

$$D_{nm} = \frac{\pi A_{nm}}{2} \left(J_{n+\frac{3}{2}}(C_\alpha) Y_{n+\frac{1}{2}}(C_\beta) - J_{n+\frac{1}{2}}(C_\alpha) Y_{n+\frac{3}{2}}(C_\beta) \right). \tag{17c}$$

We exclude the possibility that $C_\alpha = C_\beta$, as in this case the interior field would also be force free. It is worth noting that the surface toroidal field at the surface is in general non-zero, which was instead a necessary condition in the current-free case.

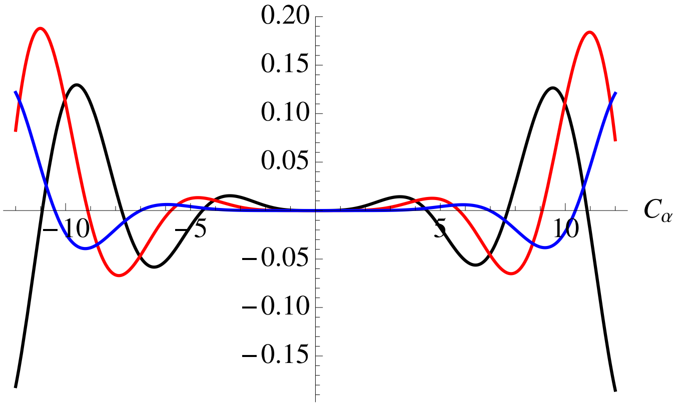

Fig. 1. Various zeroes of Eq. (19) are displayed for $R_{\rm out} = 2R$, $C_\beta = 0.1$ and $n = 1$ (black), $n = 2$ (red) and $n = 3$ (blue). The normalization is given by $A_{nm} = 1$.

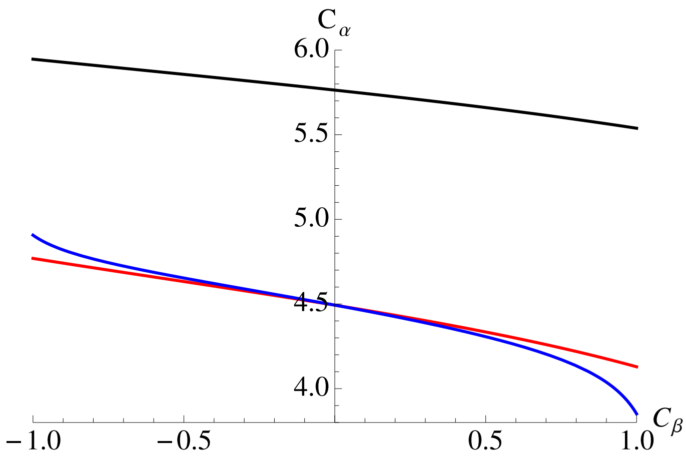

Fig. 2. Eigenvalues for the $n = 2$ (black) and for the $n = 1$ mode (red) as a function of C_β for $R_{\rm out} = 2R$. In blue we depict the $n = 1$ eigenvalue for $R_{\rm out} = 3R$.

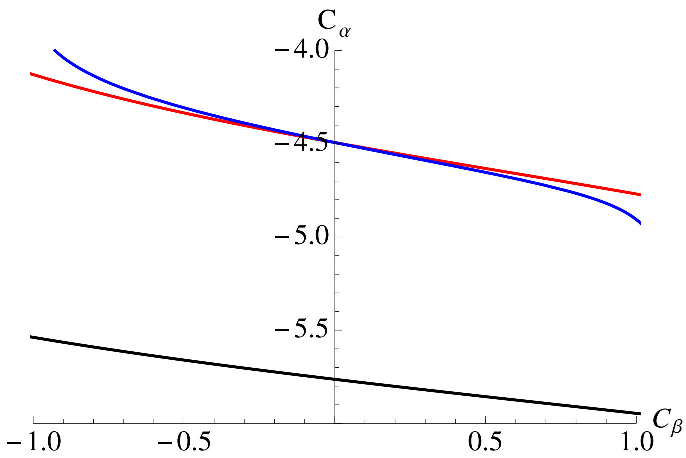

Fig. 3. Eigenvalues for the $n = 2$ (black) and for the $n = 1$ mode (red) as a function of C_β for $R_{\rm out} = 2R$ for negative values of C_α. In blue we depict the $n = 1$ eigenvalue for $R_{\rm out} = 3R$.

While in the current-free as well as in the vertical (i.e., purely radial) field case, the "quantization" condition for C_α is obtained by imposing the vanishing of the toroidal field on the stellar surface (Krause & Raedler 1980), in this case, the discrete turbulent spectrum is obtained by imposing the outer boundary condition at $r = R_{\rm out}$.

In particular, following Bonanno (2016), we assume that at $r = R_{\rm out}$ the radial component of the field is dominant, so that

$$B_\theta(r = R_{\rm out}) = B_\phi(r = R_{\rm out}) = 0. \tag{18}$$

This is consistent with the presence of a stellar wind in the solution found by Parker (1958).

It is easy to show that Eq. (18) implies the following equation to hold:

$$0 = Y_{n+\frac{1}{2}}(R_{\rm out}\beta)\left(J_{n+\frac{1}{2}}(C_\alpha)J_{n+\frac{3}{2}}(C_\beta) - J_{n+\frac{3}{2}}(C_\alpha)J_{n+\frac{1}{2}}(C_\beta)\right)$$
$$+ J_{n+\frac{1}{2}}(R_{\rm out}\beta)\left(J_{n+\frac{3}{2}}(C_\alpha)Y_{n+\frac{1}{2}}(C_\beta) - J_{n+\frac{1}{2}}(C_\alpha)Y_{n+\frac{3}{2}}(C_\beta)\right). \tag{19}$$

Clearly, the eigenvalues for a given n but different m coincide, meaning that there is degeneration with respect to m as Eq. (19) does not depend on m. It is interesting to study the "quantized" spectrum for various values of β and $R_{\rm out}$. While in the limit $\beta \to 0$ it is possible to show that Eq. (19) reproduces the well-known textbook solution for the current-free case (see Krause & Raedler 1980), in general, the β-dependence modifies the standard current-free solution.

In Fig. 1 the zeroes of Eq. (19) are displayed for $\beta = 0.1$ and $R_{\rm out} = 2R$ and various values of n, while in Figs. 2 and 3 the dependence of C_α on C_β is displayed for $n = 1$ (red) and $n = 2$ (black), while the blue line represents the $n = 1$ solution with $R_{\rm out} = 3R$.

It is clear that C_α is a decreasing function of C_β, and this pattern is substantially unchanged for any value of n. Moreover, a positive C_β produces values of C_α that are lower than in the current-free case, while negative values of C_β lead to greater values of C_α. In other words, if the current in the corona is parallel to the field, the dynamo is easily excited, while if the current is antiparallel, the dynamo condition is more difficult to attain.

Explicit values for $n = 1$ are displayed in Table 1.

The solution presented in this article in principle allows explicitly computing the magnetic helicity flux across the stellar boundary, which is non-zero for a non-vanishing C_β. The volume-integrated magnetic helicity $\boldsymbol{A} \cdot \boldsymbol{B}$ is maximum at the inner boundary, and it decays to zero at the outer boundary, as is shown in Figs. 4 and 5. This is not a coincidence: it is possible to show that our outer boundary condition (18) amounts to the condition of no helicity flux across the outer boundary.

2.3. Magnetic field components

We can provide an explicit expression for the magnetic field in the outer part of the domain.

Reality condition requires $A_{n,m} = A^*_{n,-m}$ in Eq. (17). Therefore Eq. (11) reads

$$\Phi = R\sum_{n=1}^{\infty}\sum_{m=0}^{2n}[a_n^m Q_n J_n(\beta r)\cos m\varphi$$
$$+ b_n^m S_n Y_n(\beta r)\sin m\varphi]\left(\frac{R}{r}\right)^{1/2} P_n^m(\mu), \tag{20}$$

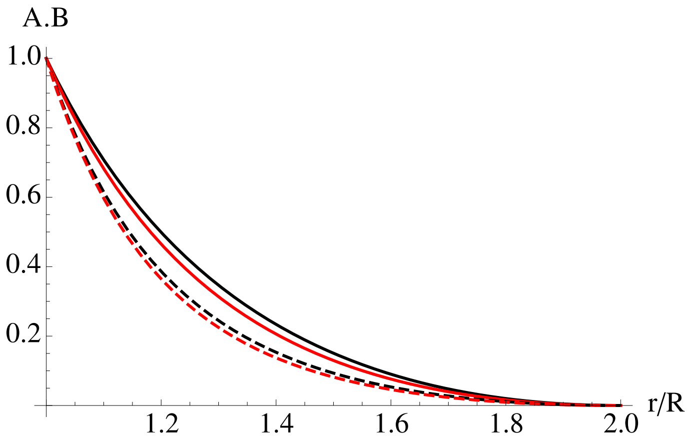

Fig. 4. Radial dependence of the magnetic helicity $\boldsymbol{A} \cdot \boldsymbol{B}$ for the $n = 1$ mode (solid line) for $C_\beta = 0.8$ (black) and $C_\beta = 0.1$ (red), and for the $n = 2$ mode (dashed lines) at $\theta = \pi/4$. The magnetic helicity is normalized using $A_{\rm nm} = 1$.

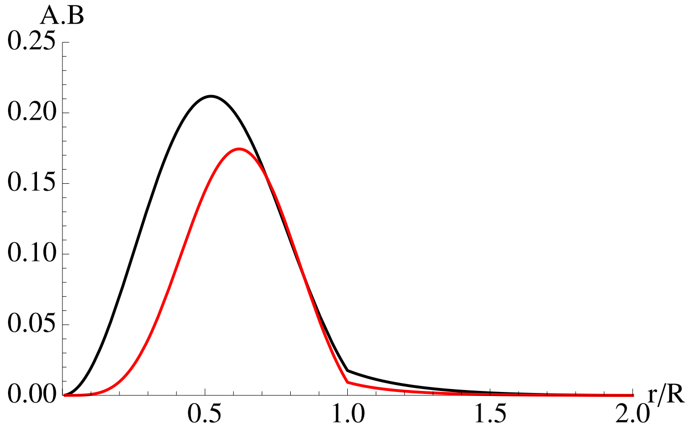

Fig. 5. Global radial dependence of the angle averaged magnetic helicity $\int \boldsymbol{A} \cdot \boldsymbol{B}\, \mathrm{d}\theta \mathrm{d}\phi$ for the $n = 1$ mode (black) mode and for the $n = 2$ mode (red) for $C_\beta = 0.5$. Note the presence of a small tail of non-zero helicity extending up to $r = 1.5R$. The magnetic helicity is normalized using $A_{\rm nm} = 1$.

Table 1. First four positive and negative eigenvalues for $n = 1$ for C_α for various values of C_β.

C_β	C_α^{11}	C_α^{12}	C_α^{13}	C_α^{14}
1	4.1290	7.3873	10.5752	13.7418
0.1	4.6384	7.6958	10.8748	14.0369
0.1	–4.5222	–7.7542	–10.9331	–14.0953
0	4.4934	7.7253	10.9041	14.0662
–0.1	4.5222	7.7542	10.9331	14.0953
–0.1	–4.6384	–7.6958	–10.8748	–14.0369
–1	4.7693	8.0139	11.1986	14.3639

Notes. We note that the invariance of the spectrum with respect to a $C_\alpha \to -C_\alpha$ and $C_\beta \to -C_\beta$ changes.

where for $\beta > 0$, a_n^m and b_n^m are arbitrary real coefficients, and

$$Q_n = J_{n+\frac{1}{2}}(C_\alpha)J_{n+\frac{3}{2}}(C_\beta) - J_{n+\frac{3}{2}}(C_\alpha)J_{n+\frac{1}{2}}(C_\beta) \tag{21}$$

$$S_n = J_{n+\frac{3}{2}}(C_\alpha)Y_{n+\frac{1}{2}}(C_\beta) - J_{n+\frac{1}{2}}(C_\alpha)Y_{n+\frac{2}{2}}(C_\beta). \tag{22}$$

Moreover, $P_n^m(\mu)$ are the normalized associated Legendre functions of degree n, order m, and argument $\mu = \cos\theta$. In particular, C_α and C_β are not arbitrary, but are linked via the quantization condition given by Eq. (19).

We thus have

$$B_r(r,\theta,\varphi) = \left(\frac{R}{r}\right)^{3/2} \sum_{n=1}^{\infty}\sum_{m=0}^{2n} \Bigg[a_n^m Q_n n(n+1) J_{n+\frac{1}{2}}(\beta r)\cos m\varphi + b_n^m S_n Y_{n+\frac{1}{2}}(\beta r)\left(n(n+1) - \frac{m^2}{\sin^2\theta}\right)\sin m\varphi \Bigg] P_n^m(\mu) \tag{23}$$

$$B_\theta(r,\theta,\varphi) = \frac{1}{2}\left(\frac{R}{r}\right)^{3/2} \sum_{n=1}^{\infty}\sum_{m=0}^{2n} \Bigg[-2a_n^m Q_n r\beta J_{n+\frac{1}{2}}(\beta r)\frac{m}{\sin\theta}\sin m\varphi P_n^m(\mu) + a_n^m Q_n \left[J_{n+\frac{1}{2}}(\beta r) + 2r\frac{\mathrm{d}}{\mathrm{d}r}J_{n+\frac{1}{2}}(\beta r)\right]\cos m\varphi \frac{d}{d\theta}P_n^m(\mu) + b_n^m S_n\left[Y_{n+\frac{1}{2}}(\beta r) + 2r\frac{\mathrm{d}}{\mathrm{d}r}Y_{n+\frac{1}{2}}(\beta r)\right]\sin m\varphi\frac{d}{d\theta}P_n^m(\mu)\Bigg] \tag{24}$$

$$B_\phi(r,\theta,\varphi) = -\frac{1}{2}\left(\frac{R}{r}\right)^{3/2} \sum_{n=1}^{\infty}\sum_{m=0}^{2n} \Bigg[2a_n^m Q_n \left[J_{n+\frac{1}{2}}(\beta r) + 2r\frac{\mathrm{d}}{\mathrm{d}r}J_{n+\frac{1}{2}}(\beta r)\right]\frac{m}{\sin\theta}\sin m\varphi P_n^m(\mu) + \left(2\beta r a_n^m Q_n J_{n+\frac{1}{2}}(\beta r)\cos m\varphi + b_n^m S_n Y_{n+\frac{1}{2}}(\beta r)\sin m\varphi\right)\frac{\mathrm{d}}{\mathrm{d}\theta}P_n^m(\mu)\Bigg]. \tag{25}$$

3. Conclusion

The analytical linear force-free solution presented in this paper has been obtained by coupling a corona with a dynamo-generated field in the interior. Although it is a highly idealized situation, it shows several interesting features. The most important property of the solution is the endowment of a new dependence of the dynamo number on the strength and the topology of the force-free field as parametrized by the parameter β. Positive β produces smaller dynamo numbers, while negative β renders the dynamo more difficult to excite. This is in agreement with the harmonic atmosphere model in Bonanno (2016), as Beltrami fields are also harmonic, while the reverse is not true in general. The toroidal field is non-zero at the surface, and therefore it could be important to implement this solution in the ZDI regularization procedure. Because the coupling with the interior has significantly reduced the number of free parameters that are required to specify the field for each harmonics, the space of possible solutions could be significantly reduced. We hope to discuss possible physical application of our solution in a forthcoming paper, where we will extend our approach to the non-stationary dynamo case.

Acknowledgements. We thank Axel Brandenburg for comments and useful discussions. F.D.S. acknowledges the Swedish Research Council International Postdoc fellowship for support, Giuseppe Jacopo Guidi for discussions, and the INAF Astrophysical observatory of Catania for the warm hospitality that allowed this work to be carried out.

References

Bonanno, A. 2016, ApJ, 833, L22
Carroll, T. A., Kopf, M., Strassmeier, K. G., & Ilyin, I. 2009, in Cosmic Magnetic Fields: From Planets, to Stars and Galaxies, eds. K. G. Strassmeier, A. G. Kosovichev, & J. E. Beckman, IAU Symp., 259, 633
Chandrasekhar, S., & Kendall, P. C. 1957, ApJ, 126, 457
Chandrasekhar, S., & Woltjer, L. 1958, Proceedings of the National Academy of Science, 44, 285
Krause, F., & Raedler, K.-H. 1980, Mean-field magnetohydrodynamics and dynamo theory (Pergamon Press)
Moffatt, H. K. 1980, Magnetic field generation in electrically conducting fluids (Moskva: Mir)
Nakagawa, Y. 1973, A&A, 27, 95
Nash, A. G., Sheeley, Jr., N. R., & Wang, Y.-M. 1988, Sol. Phys., 117, 359
Parker, E. N. 1958, ApJ, 128, 664
Priest, E. R. 1982, Solar magneto-hydrodynamics (Dordrecht, The Netherlands: D. Reidel Pub. Co.)
Proctor, M., & Gilbert, A. 1994, Lectures on Solar and Planetary Dynamos (Cambridge University Press)
Stift, M. J., & Leone, F. 2017, ApJ, 834, 24
Warnecke, J., Brandenburg, A., & Mitra, D. 2011, A&A, 534, A11
Warnecke, J., Brandenburg, A., & Mitra, D. A. 2012, Journal of Space Weather and Space Climate, 2, A11
Warnecke, J., Käpylä, P. J., Käpylä, M. J., & Brandenburg, A. 2016, A&A, 596, A115
Wiegelmann, T., & Sakurai, T. 2012, Liv. Rev. Sol. Phys., 9, 5